

# Semiconducting hexagonal boron nitride for deep ultraviolet photonics

S. Majety, X. K. Cao, R. Dahal, B. N. Pantha, J. Li, J. Y. Lin<sup>a)</sup> and H. X. Jiang<sup>a)</sup>

Department of Electrical and Computer Engineering, Texas Tech University, Lubbock, TX  
79409

## ABSTRACT

Hexagonal boron nitride (hBN) has been recognized as an important material for various device applications and as a template for graphene electronics. Low-dimensional hBN is expected to possess rich physical properties, similar to graphene. The synthesis of wafer-scale semiconducting hBN epitaxial layers with high crystalline quality and electrical conductivity control is highly desirable. We report the successful synthesis of large area hBN epitaxial layers (up to 2-inch in diameter) by metal organic chemical vapor deposition. P-type conductivity control was also attained by in-situ Mg doping. Compared to Mg doped wurtzite AlN, which possesses a comparable energy band gap (~6 eV), dramatic reductions in Mg acceptor energy level and p-type resistivity have been realized in hBN epilayers. Our results indicate that (a) hBN epitaxial layers exhibit outstanding semiconducting properties and (b) hBN is the material of choice for DUV optoelectronic devices. The ability of conductivity control and wafer-scale production of hBN opens up tremendous opportunities for emerging applications, ranging from revolutionizing p-layer approach in III-nitride deep ultraviolet optoelectronics to graphene electronics.

Key words: Hexagonal boron nitride, wide bandgap semiconductors, p-type conductivity control, deep UV photonics, graphene electronics.

## 1. INTRODUCTION

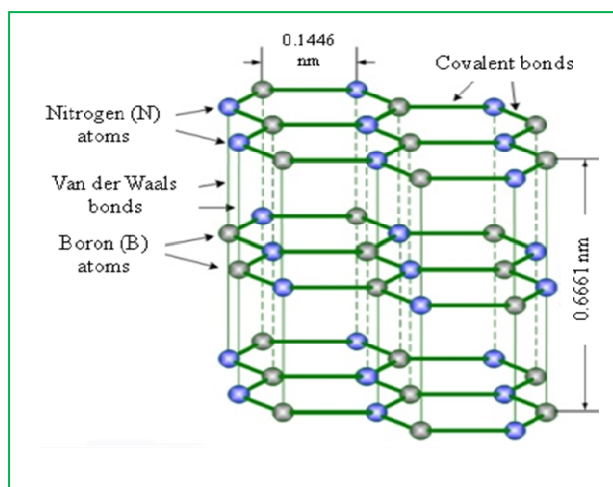


Fig. 1 Schematic of hexagonal boron nitride (h-BN) structure

Among the members of the III-nitride material system, boron nitride having a band gap comparable to AlN ( $E_g \sim 6$  eV), is the least studied and understood.<sup>1-8</sup> Due to its extraordinary physical properties, such as high chemical stability, thermal conductivity, melting temperature, electrical resistivity, and band gap, BN appears to be the material of choice for emerging applications, including deep UV (DUV) optoelectronics. In particular, as shown in Fig. 1, hexagonal boron nitride (hBN) has a close lattice match to graphene and is the most suitable substrate and dielectric/separation layer for graphene electronics and optoelectronics.<sup>9-11</sup> Similar to graphene, low dimensional hBN is expected to possess rich new physics.

Due to its high bandgap and in-plane thermal conductivity, hBN has been considered both as an excellent electrical insulator and thermal conductor. However, lasing action in deep ultraviolet (DUV) region ( $\sim 225$  nm) by electron beam excitation was demonstrated in small hBN bulk crystals synthesized by a high pressure/temperature technique,<sup>12</sup> raising its promise as a semiconducting material for realizing chip-scale DUV light sources/sensors. So far, hBN bulk crystals with size up to millimeters can be grown. Other than small size, bulk crystal growth has disadvantages of difficulty to control growth conditions such as intentional doping and formation of quantum well based device structures and is more suitable for synthesizing bulk crystals as substrates. The synthesis of wafer-scale semiconducting hBN epitaxial layers with high crystalline quality and electrical conductivity control has not been previously achieved, but is highly desirable for the fundamental understanding and the exploration of emerging applications of this interesting material.

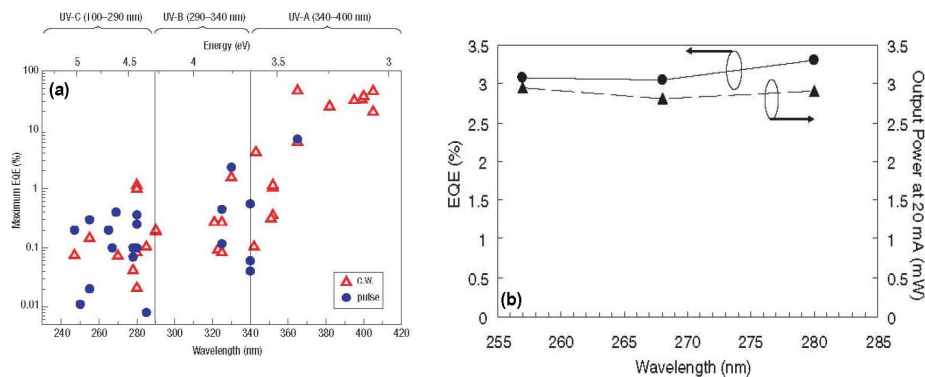


Fig. 2 (a) External quantum efficiencies (EQE) of UV LEDs attained by various research groups,<sup>13</sup> (b) Maximum EQE and output power at 20 mA for 257, 268, and 280 nm of best DUV LED devices.<sup>14</sup>

Meanwhile, in the last decade, there have been significant advances in the area of III-nitride materials and device technologies. However, as illustrated in Fig. 2 (a), the quantum efficiency of AlGaIn based DUV ( $\lambda < 280$  nm) light emitting diodes (LEDs) decreases exponentially with a decrease in emission wavelength.<sup>13</sup> Figure 2(b) shows that the quantum efficiency of current state-of-the-art DUV LEDs is limited to around 3% at 280 nm.<sup>14</sup> DUV ( $\lambda < 280$  nm) devices are highly useful in areas such as probing intrinsic fluorescence in a protein, equipment/personnel decontamination, and photocatalysis.<sup>13</sup> The most outstanding issue for realizing DUV light emitting devices with high QE is the low conductivity of p-type AlGaIn.

Our group has determined the acceptor energy levels of Mg ( $\sim 0.5$  eV) and Zn ( $\sim 0.6$  eV) in AlN.<sup>15-19</sup> We found that the Mg acceptor level ( $E_A$ ) in  $Al_xGa_{1-x}N$  increases with  $x$ , from about 170 meV in GaN ( $x=0$  with  $E_g \sim 3.4$  eV) to 510 meV in AlN ( $x=1$  with  $E_g \sim 6.1$  eV),<sup>15-18</sup> as illustrated in Fig. 3(a). The free hole concentration ( $p$ ) decreases with the acceptor activation energy following  $p \sim \exp(-E_A/kT)$ . As a result, the free hole concentration decreases exponentially with a decrease in emission wavelength (or increase in bandgap), as shown in Fig. 3(b). An  $E_A$  value around 500 meV in AlN translates to only 1 free hole for roughly every 2 billion ( $2 \times 10^9$ ) incorporated Mg impurities at room temperature. This leads to extremely resistive p-layers. For instance, an optimized Mg doped AlN epilayer has a typical “p-type resistivity” of  $> 10^7 \Omega \cdot \text{cm}$  at 300 K.<sup>17-18</sup> This causes an extremely low free hole injection efficiency into the quantum well active region and is a major obstacle for the realization of AlGaIn-based DUV light emitting devices with

high QE. Currently, the highest QE of AlGa<sub>x</sub>N based DUV ( $\lambda < 280$  nm) LED is around 3%.<sup>14</sup> It should be noted that the deepening of the Mg acceptor level in Al<sub>x</sub>Ga<sub>1-x</sub>N with increasing x is a fundamental physics problem.

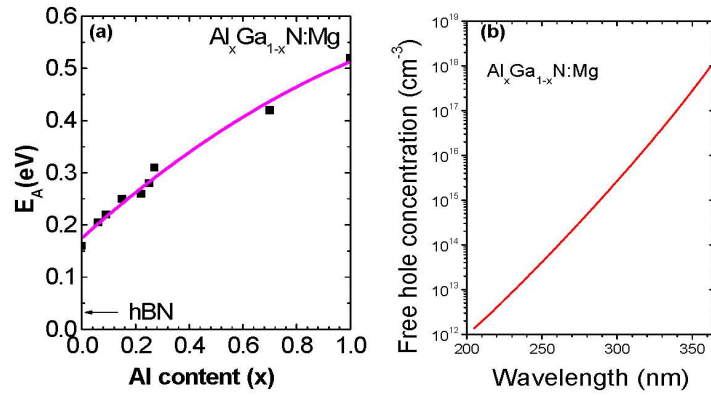


Fig. 3 (a) Mg acceptor level ( $E_A$ ) in AlGa<sub>x</sub>N and the arrow indicates measured  $E_A$  value in a Mg doped hBN epilayer.<sup>15-20</sup> (b) Free hole concentration as a function of the emission wavelength of Al<sub>x</sub>Ga<sub>1-x</sub>N DUV LEDs. In the plot, we used  $E_g(x) = xE_g(\text{AlN}) + (1-x)E_g(\text{GaN}) + bx(1-x)$ ,  $E_g(\text{AlN})=6.05\text{eV}$ ,  $E_g(\text{GaN})=3.42\text{eV}$ ,  $b=0.98\text{eV}$  and the typical free hole concentration of Mg doped GaN,  $p_{\text{GaN}}=1 \times 10^{18} \text{cm}^{-3}$ .

## 2. EXPERIMENT

Hexagonal BN epitaxial layers were synthesized by metal organic chemical vapor deposition (MOCVD) using triethylboron (TEB) source and ammonia (NH<sub>3</sub>) as B and N precursors, respectively.<sup>20</sup> Prior to epilayer growth, a 20 nm BN or AlN buffer layer was first deposited on sapphire substrate at 800 °C. The typical hBN epilayer growth temperature was about 1300 °C. For the growth of Mg doped hBN, biscyclopentadienyl-magnesium was transported into the reactor during hBN epilayer growth. Mg-doping concentration in the epilayers used in this study was about  $1 \times 10^{19} \text{cm}^{-3}$ , as verified by secondary ion mass spectrometry (SIMS) measurement (performed by Charles and Evan). X-ray diffraction (XRD) was employed to determine the lattice constant and crystalline quality of the epilayers. Photoluminescence (PL) properties were measured by a DUV laser spectroscopy system.<sup>21</sup> Hall-effect and standard Van der Pauw measurements were employed to measure the hole concentration and mobility and electrical conductivity. Seebeck effect (or hot probe) measurement was performed to further verify the conductivity type.

## 3. RESULTS AND DISCUSSION

XRD  $\theta$ - $2\theta$  scan shown in Fig. 4(a) revealed a  $c$ -lattice constant  $\sim 6.67 \text{ \AA}$ , which closely matches to the bulk  $c$ -lattice constant of h-BN ( $c=6.66 \text{ \AA}$ ),<sup>1,2,6,22</sup> affirming that BN films are of single *hexagonal* phase. Figure 4(b) is the XRD rocking curve of the (0002) reflection of a 1  $\mu\text{m}$  thick film. The observed linewidth is comparable to those of typical GaN epilayers grown on sapphire with a similar thickness.<sup>23</sup> This signifies that these hBN epilayers are of relatively high crystalline quality. SIMS measurement results shown in Fig. 5(a) revealed that hBN epilayers have excellent stoichiometry.

Figure 5(c) compares low temperature (10 K) deep UV PL spectra of hBN and AlN. hBN exhibits a dominant emission line at  $\sim 5.46 \text{ eV}$ . An interesting observation is that its emission intensity is more than 2 orders of magnitude stronger than the dominant band-edge emission of a high quality AlN epilayer.<sup>20</sup> This strong intensity may be related in part to the high band-edge optical absorption coefficient in hBN ( $> 5 \times 10^5 \text{ cm}^{-1}$ ).<sup>4,24</sup>

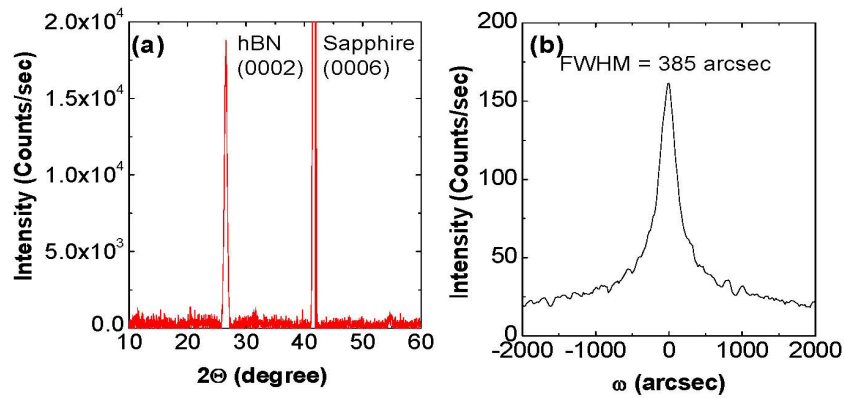


Fig. 4 XRD measurement results of an hBN epilayer: (a)  $\theta$ - $2\theta$  scan and (b) rocking curve of the (0002) reflection.

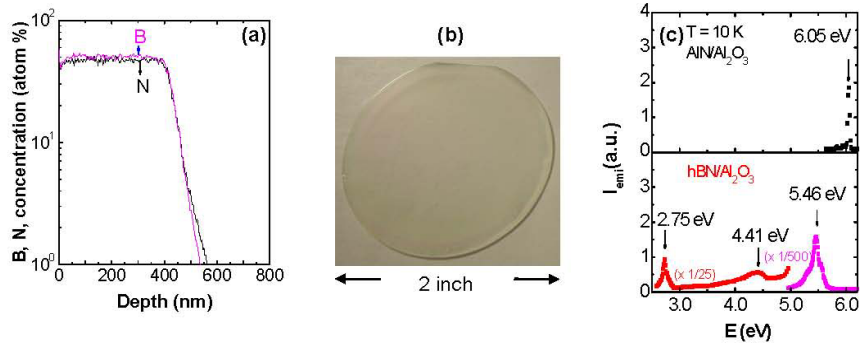


Fig. 5 (a) SIMS measurement results of an hBN epilayer. (b) A micrograph of a 2-inch hBN epilayer wafer grown on sapphire substrate. (c) Deep UV PL spectra of hBN and AlN measured at 10 K.

One of the most significant differences between AlN and hBN is the lower acceptor energy level in hBN than in AlN. In contrast to the AlN, Hall effect measurement results shown in Fig. 6 indicate that Mg doped hBN (hBN:Mg) exhibits a p-type resistivity around  $12 \Omega\cdot\text{cm}$  at 300 K. The estimated  $E_A$  value in hBN:Mg is around 31 meV based on the temperature dependent resistivity measurement. This value of  $E_A$  is lower than previously determined acceptor levels ranging from 150 -300 meV in BN films containing mixed cBN/hBN phases grown by evaporation and sputtering techniques.<sup>25-27</sup> Hall-effect measurements revealed a free hole concentration  $p \sim 1.1 \times 10^{18} \text{ cm}^{-3}$  and mobility  $\mu \sim 0.5 \text{ cm}^2/\text{V}\cdot\text{s}$ . Based on the measured  $E_A$  value of 31 meV and Mg doping concentration of  $1 \times 10^{19} \text{ cm}^{-3}$ , the expected fraction of acceptor activation and  $p$  value at 300 K would be about 30% and  $3 \times 10^{18} \text{ cm}^{-3}$ , respectively. Thus, the measured and expected  $p$  values are in a reasonable agreement. We expect the measured  $p$  to be lower than the value estimated from acceptor activation since our hBN:Mg epilayers still possess appreciable concentrations of defects (including free hole compensating centers), as indicated in PL spectrum in Fig. 5(c).

Due to the low hole mobility of our current Mg doped hBN epilayers, we also performed Seebeck effect measurement to further confirm the conductivity type. Seebeck effect measurement is a well established technique to distinguish between  $n$ -type and  $p$ -type conductivity of a semiconductor.<sup>28</sup> A schematic illustration of the experimental set-up for the Seebeck effect measurement is shown in Fig. 7(a). The samples were cut into a rectangular shape ( $\sim 5 \times 20 \text{ mm}^2$ ). One end of the sample was placed on the sink while a heater was attached on the other end. On the surface of the sample, two thermocouples separated by  $\sim 8 \text{ mm}$  were attached. An in-plane temperature gradient was created along the sample by the heater. The

temperature gradient created a voltage between the cold and hot ends due to the diffusion of thermally excited charged carriers. The direction of this induced potential gradient relative to the direction of the temperature gradient can be utilized to determine if the material is p- or n-type. As an illustration, the Seebeck voltage and temperature gradients were measured for a hBN:Mg sample against a standard n-type  $\text{In}_{0.3}\text{Ga}_{0.7}\text{N}:\text{Si}$  reference sample and the results are shown in Fig. 7(b) [20]. The Seebeck coefficient for Si doped  $\text{In}_{0.3}\text{Ga}_{0.7}\text{N}$  was  $S = \Delta V/\Delta T + S_{\text{Alumel}} = -42.2 - 18.5 = -60.7 \mu\text{V}/\text{K}$ , while for Mg doped hBN was  $S = \Delta V/\Delta T + S_{\text{Alumel}} = 28.0 - 18.5 = 9.5 \mu\text{V}/\text{K}$ . The sign reversal in  $S$  over n-type  $\text{In}_{0.3}\text{Ga}_{0.7}\text{N}:\text{Si}$  sample confirms unambiguously that hBN:Mg epilayers are p-type.

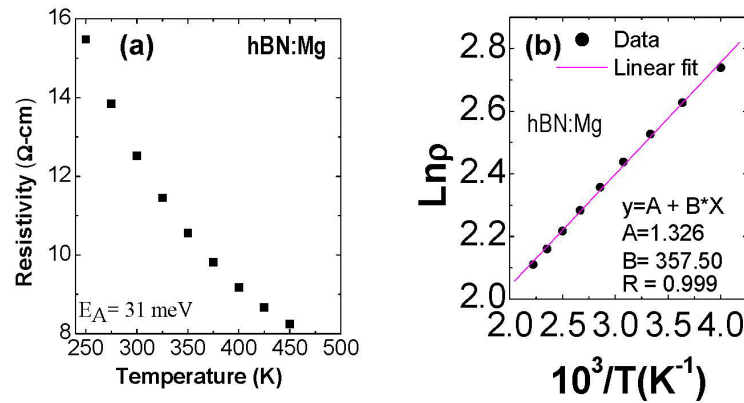


Fig. 6 p-type resistivity as a function of temperature of an hBN:Mg epilayer in (a) linear scale and (b) semi-log plot.

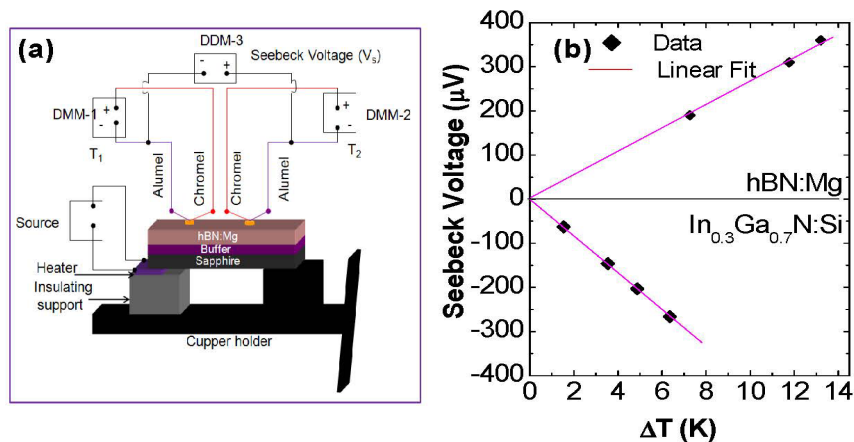


Fig. 7 (a) Schematic of experimental set-up of Seebeck effect measurement. (b) Seebeck coefficients of Mg doped hBN (hBN:Mg) and n-type  $\text{In}_{0.3}\text{Ga}_{0.7}\text{N}:\text{Si}$  (with  $n = 3 \times 10^{19} \text{ cm}^{-3}$  and  $\mu = 90 \text{ cm}^2/\text{V}\cdot\text{s}$ ).<sup>20</sup>

#### **4. SUMMARY**

Further works are needed to further improve the overall material quality (and hence hole mobility) and understanding of the mechanisms for defect generation and elimination. Nevertheless, the dramatic reduction in  $E_A$  and p-type resistivity (by about 6-7 orders of magnitude) of hBN over AlN:Mg represents an exceptional opportunity to revolutionize p-layer approach and overcome the intrinsic problem of p-type doping in Al-rich AlGaN, thus potentially providing significant enhancement to the QE of DUV devices.

#### **ACKNOWLEDGEMENTS**

The work dealing with p-type doping issue in III-nitrides is support by DARPA's Compact Mid-Ultraviolet Technology (CMUVT) program (managed by Dr. John Albrecht). The hexagonal boron nitride epi-growth work is also supported in part by DHS managed by Dr. Mark Wrobel (grant number 2011-DN-077-ARI048-02). Jiang and Lin are grateful to the AT&T Foundation for the support of Ed Whitacre and Linda Whitacre Endowed chairs.

## REFERENCES

- a) [hx.jiang@ttu.edu](mailto:hx.jiang@ttu.edu); [jingyu.lin@ttu.edu](mailto:jingyu.lin@ttu.edu)
- [1] Siklitsky, V., "Boron Nitride," <http://www.ioffe.rssi.ru/SVA/NSM/Semicond/BN/index.html>.
- [2] Rumyantsev, S. L., Levinshtein, M. E., Jackson, A. D., Mohammad, S. N., Harris, G. L., Spencer, M. G., Shur, M. S., [Properties of Advanced Semiconductor Materials GaN, AlN, InN, BN, SiC, SiGe], John Wiley & Sons, Inc., New York, 67-92 (2001).
- [3] Kubota, Y., Watanabe, K., Tsuda, O. and Taniguchi, T., "Deep Ultraviolet Light-Emitting Hexagonal Boron Nitride Synthesized at Atmospheric Pressure," *Science*, 317(5840), 932-934 (2007).
- [4] Sugino, T., Tanioka, K., Kawasaki, S. and Shirafuji, J., "Characterization and field emission of sulfur-doped boron nitride synthesized by plasma-assisted chemical vapor deposition," *Jpn. Appl. Phys.*, 36, L463 (1997).
- [5] Landolt-Bornstein, edited by Madelung, O., [Numerical Data and Functional Relationship in Science and Technology—Crystal and Solid State Physics], Vol. III, Springer, Berlin, (1972).
- [6] Pease, R. S., "An X-ray study of boron nitride," *Acta Cryst.*, 5, 356-361 (1952).
- [7] Rubio, A., Corkill, J. L. and Cohen, M. L., "Theory of graphitic boron nitride nanotubes," *Phys. Rev. B* 49(7), 5081-5084 (1994).
- [8] Chopra, N. G., Luyken, R. J., Cherrey, K., Crespi, V. H., Cohen, M. L., Louie, S. G. and Zettl, A., "Boron-Nitride Nanotubes," *Science*, 269(18), 966-967 (1995).
- [9] Song, L., Ci, L., Lu, H., Sorokin, P. B., Jin, C., Ni, J., Kvashnin, A. G., Kvashnin, D. G., Lou, J., Yakobson, B. I., and Ajayan, P. M., "Large Scale Growth and Characterization of Atomic Hexagonal Boron Nitride Layers," *Nano Lett.*, 10(8), 3209-3215 (2010).
- [10] Alem, N., Erni, R., Kisielowski, C., Rossell, M. D., Gannett, W. and Zettl, A., "Atomically thin hexagonal boron nitride probed by ultrahigh-resolution transmission electron microscopy," *Phys. Rev. B*, 80(15), 155425 (2009).
- [11] Dean, C. R., Young, A. F., Meric, I., Lee, C., Wang, L., Sorgenfrei, S., Watanabe, K., Taniguchi, T., Kim, P., Shepard, K. L. and Hone, J., "Boron nitride substrates for high-quality graphene electronics," *Nature Nanotechnology*, 5(10), 722-726 (2010).
- [12] Watanabe, K., Taniguchi, T. and Kanda, H., "Far-ultraviolet plane-emission handheld device based on hexagonal boron nitride," *Nature Photonics*, 3(10), 591-594 (2009).
- [13] Khan, A., Balakrishnan, K. and Katona, T., "Ultraviolet light-emitting diodes based on group three nitrides," *Nature Photonics* 2(2), 77-84 (2008).
- [14] Pernot, C., Kim, M., Fukahori, S., Inazu, T., Fujita, T., Nagasawa, Y., Hirano, A., Ippommatsu, M., Iwaya, M., Kamiyama, S., Akasaki, I., and Amano, H., "Improved Efficiency of 255–280 nm AlGaIn-Based Light-Emitting Diodes," *Appl. Phys. Express*, 3(6), 061004 (2010).
- [15] Nakarmi, M. L., Kim, K. H., Khizar, M., Fan, Z. Y., Lin, J. Y. and Jiang, H. X., "Electrical and optical properties of Mg-doped Al<sub>0.7</sub>Ga<sub>0.3</sub>N alloys," *Appl. Phys. Lett.*, 86(9), 092108 (2005).
- [16] Nam, K.B., Nakarmi, M. L., Li, J., Lin, J. Y. and Jiang, H. X., "Mg Acceptor Level in AlN Probed by Deep Ultraviolet Photoluminescence," *Appl. Phys. Lett.*, 83(5), 878 (2003).
- [17] Nakarmi, M. L., Nepal, N., Ugolini, C., Al Tahtamouni, T. M., Lin, J. Y. and Jiang H. X., "Correlation between optical and electrical properties of Mg-doped AlN epilayers," *Appl. Phys. Lett.*, 89(15), 152120 (2006).
- [18] Nakarmi, M. L., Nepal, N., Lin, J. Y. and Jiang, H. X., "Photoluminescence studies of impurity transitions in Mg-doped AlGaIn alloys," *Appl. Phys. Lett.*, 94(9), 091903 (2009).
- [19] Nepal, N., Nakarmi, M. L., Jang, H. U., Lin, J. Y. and Jiang, H. X., "Growth and photoluminescence studies of Zn-doped AlN epilayers," *Appl. Phys. Lett.*, 89(19), 192111 (2006).
- [20] Dahal, R., Li, J., Majety, S., Pantha, B. N., Cao, X. K., Lin, J. Y., and Jiang, H. X., "Epitaxially grown semiconducting hexagonal boron nitride as a deep ultraviolet photonic material," *Appl. Phys. Lett.*, 98(21), 211110 (2011).
- [21] <http://www2.ece.ttu.edu/Nanophotonics/>.
- [22] Lynch, R. W., and Drickamer, H. G., "Effect of High Pressure on the Lattice Parameters of Diamond, Graphite, and Hexagonal Boron Nitride," *J. Chem. Phys.*, 44(1), 181 (1966).

- [23] Nakamura, S., Fasol, G., and Pearton, S. J., [The blue laser diode: the complete story], Springer, Berlin, (2000).
- [24] Zunger, A., Katzir, A., and Halperin, A., "Optical properties of hexagonal boron nitride," *Phys. Rev. B*, 13(12), 5560-5573 (1976).
- [25] Lu, M., Bousetta, A., Bensaoula, A., Waters, K., and Schultz, J. A., "Electrical properties of boron nitride thin films grown by neutralized nitrogen ion assisted vapor deposition," *Appl. Phys. Lett.*, 68(5), 622 (1996).
- [26] Nose, K., Oba, H. and Yoshida, T., "Electric conductivity of boron nitride thin films enhanced by in situ doping of zinc," *Appl. Phys. Lett.*, 89(11), 112124 (2006).
- [27] He, B., Zhang, W. J., Yao, Z. Q., Chong, Y. M., Yang, Y., Ye, Q., Pan, X. J., Zapien, J. A., Bello, I., Lee, S. T., Gerhards, I., Zutz, H. and Hofsass, H., "p-type conduction in beryllium-implanted hexagonal boron nitride films," *Appl. Phys. Lett.*, 95(25), 252106 (2009).
- [28] Van Zeghbroeck, B., [Principles of Semiconductor Devices], Univ. of Colorado, Boulder CO, Chap. 2 (2007).